Highlights on Spanish Astrophysics X, Proceedings of the XIII Scientific Meeting of the Spanish Astronomical Society held on July 16 – 20, 2018, in Salamanca, Spain. B. Montesinos, A. Asensio Ramos, F. Buitrago, R. Schödel, E. Villaver, S. Pérez-Hoyos, I. Ordóñez-Etxeberria (eds.), 2019

Self-consistent spatially-resolved star formation histories of 2 < z < 3 galaxies from CANDELS.

Ángela García Argumánez[1], Pablo G. Pérez-González[1,2], Armando Gil de Paz[1], and Javier Gorgas[1]

[1] Departamento de Física de la Tierra y Astrofísica, Universidad Complutense de Madrid, Plaza Ciencias, 1, E-28040 Madrid, Spain
[2] Centro de Astrobiología (CAB, INTA-CSIC), Carretera de Ajalvir km 4, E-28850 Torrejón de Ardoz, Madrid, Spain

Abstract

In order to shed new light on how Milky Way-like galaxies are formed, we analyze the star formation histories (SFHs) and mass surface density profiles of massive galaxies ($\log(M_*/M_\odot) > 10$) at $2 < z < 3$ in the GOODS-N and GOODS-S fields observed by the Cosmic Assembly Near-infrared Deep Extragalactic Legacy Survey (CANDELS). Stellar population parameters are obtained in two-dimensions (2D) by first performing multi-wavelength photometry using optical and near-infrared broad-band data from HST. Subsequently, the observed SEDs are fit to stellar population models attenuated by dust. The galaxy sample has been divided according to its activity (star-forming vs. quiescent) and compactness (compact vs. extended). We will discuss the differences in SFH and mass distribution for each subsample and propose an evolutionary connection among them.

1 Introduction

In general, galaxies increase their mass by gas accretion, travelling within the Main Sequence [10] until stellar formation ceases because of some feedback mechanism or by gas depletion. At that moment, they reach a quiescent state, in which their mass might continue increasing by dry mergers. Nevertheless, we know there is a significant number of massive quiescent galaxies already in place at high redshift, without any stellar formation [5], [6], and whose number densities are a challenge to galaxy formation models [11], [9]. Understanding the evolution between star-forming and quiescent galaxies is essential to improve our comprehension of feedback processes in massive star-forming galaxies and the evolution of galaxies in general.

In this contribution we will introduce the first preliminary results of our study, intended to establish an evolutionary connection between massive star-forming and quiescent galaxies at high redshift. To do so, we will analyse the stellar populations in 2D of massive galaxies at $2 < z < 3$ using multi-wavelength photometry. We will also briefly introduce our ongoing work focused on improving our analysis by taking into account photometric data with different spatial resolution.

1.1 Massive galaxy formation and analysis plan

Massive quiescent galaxies are supposed to be formed by two different mechanisms: a fast track, through which massive Star-Forming (SF) Galaxies at $z \gtrsim 2$ first evolve to a compact starbursting remnant (or blue nugget) by usually very fast, violent, dissipative processes. Then, the subsequent star-formation quenching in these compact star-forming galaxies transforms them into compact quiescent galaxies (or red nuggets), which increase their size afterwards by dry mergers and abandon the compact region by $z \sim 1$. Alternatively, there is also a slow track at $z \lesssim 2$, through which normal-sized SF galaxies populate the red sequence by secular evolution. Fig. 1 shows an schematic view of these two mechanisms [1].

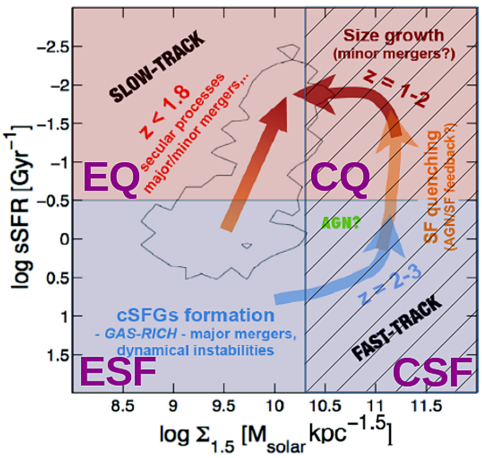

Figure 1: Figure adapted from Barro et al. [1] that shows an schematic view of the two different ways through which massive quiescent galaxies are formed: early and fast tracks. The black contour shows the galaxy distribution at low redshift. The four quadrants in the figure correspond to the galaxy types in our classification: ESF (extended star-forming), CSF (compact star-forming), EQ (extended quiescent) and CQ (compact quiescent) galaxies.

Our work focuses on studying whether there is a link among galaxy types in the fast track by analysing their stellar population and morphological properties. In particular, we will do that by analysing stellar masses and densities to understand the assembly of structures and the recent star formation locally on star-forming galaxies. Our approach to the problem includes the study of the global Star Formation Histories (SFHs) of different types of galaxies (according to their morphology and star formation activity), the analysis of their averaged surface stellar density profiles and the study of the spatially resolved stellar populations properties. Directly related to this goal, we will also try to understand the intrinsic and typical degeneracies of stellar populations synthesis studies.

2 2D stellar population analysis

The initial galaxy sample was built using the CANDELS/F160W catalog in the GOODS-S field only considering massive galaxies ($M > 10^{10}$ $M_{\odot}$) at $2 < z < 3$. These galaxies were classified into the three subsamples of interest according to their activity (star-forming vs. quiescent) and compactness (compact vs. extended): ESF (extended star-forming), CSF (compact star-forming) and CQ (compact quiescent) galaxies. Quiescent and star-forming galaxies are differentiated by a cut in specific SFR (sSFR) in $10^{-0.5}$ Gyr^{-1}. Compact galaxies are defined like [1] as those with $\Sigma_{1.5} \equiv M/r_{\rm eff}{}^{1.5} > 10^{10.3}$ $M_{\odot}$ kpc$^{-1.5}$. Fig. 2 shows this classification.

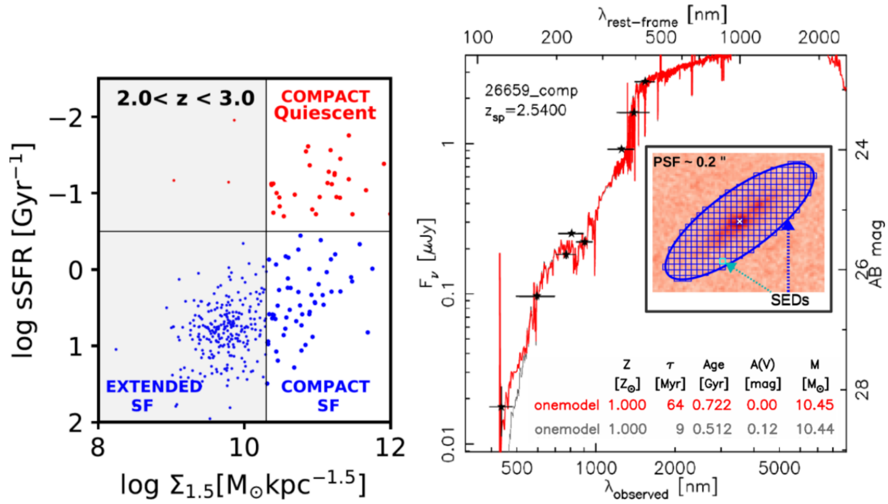

Figure 2: *Left:* selection of our sample and classification. The black lines define the selection criteria for star-forming (blue) and quiescent (red) galaxies, and for compact and extended (shaded area). *Right:* example of a Spectral Energy Distribution (SED) that has two possible clusters of solutions in the age-τ plane. The red fit corresponds to the median values of the most significant cluster of the elliptical aperture in the inset (92% of the simulated solutions belong to this cluster).

Photometry was measured using nine broad-band visible and near-infrared HST filters: F435W, F606W, F775W, F814W and F850LP in the ACS/WFC [8], and F105W, F120W, F140W and F160W in the WFC3 [7]. Photometry was measured on each galaxy inside an aperture defined by its Kron radius and using a grid with size equal to $0.2''$.

The SEDs were compared with the stellar population models of Bruzual & Charlot (2003) [2], assuming a Chabrier (2003) IMF [4] and a Calzetti (2000) attenuation law [3]. For the SFH, we assumed a time-delayed exponential with a τ star formation timescale, $SFR(t) \propto t \cdot e^{-t/\tau}$. Our modelling assumed solar metallicity. We set as free parameters the masses, ages, τ and $A(V)$. To study degeneracies, Montecarlo simulations were performed for each galaxy by allowing the photometric data to randomly vary within their photometric error and then refitting. The clustering of the solutions in the age-τ plane provided us with information about what degeneracies we had and about the uncertainty of our solutions. Fig. 2 *right* shows an example of a SED-fit with two different clusters in this plane.

3 Surface stellar density profiles of CQ, CSF and ESF galaxies

Once stellar masses were calculated for different regions in each galaxy, azimutally averaged surface stellar density profiles were built. Then, we produced average profiles for the different types of galaxy. Fig. 3 shows the median profiles for the three subsamples. The shaded areas include 68% of the values. Median surface density values as a function of radius for each galaxy are also depicted. At the bottom, we show the median profiles normalized by their maximum value and fit to a Sérsic law [12]. CQ and CSF galaxies show very similar profiles and are more concentrated than those of ESF galaxies. Additionally, the mass density profiles for compact galaxies (either quiescent or star-forming) are well described by only one Sérsic law. This can be interpreted as both types of galaxies having only one mass component, probably a bulge.

Concerning ESF galaxies, only one Sérsic component is not enough to describe the mass profile. It can be noticed that while the outer part of the curve could be explained by an exponential disc, the inner part is better described by the combination of this exponential component and a second Sérsic component. A possible explanation for that is the presence of a bulge which is being formed.

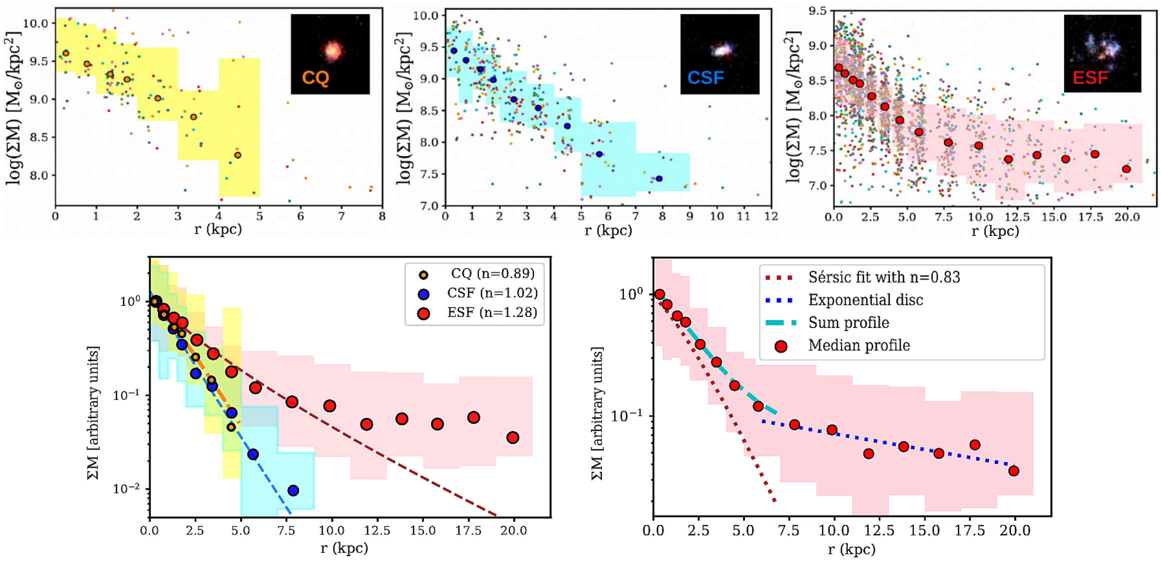

Figure 3: *Top:* surface stellar density profiles for CQ (left), CSF (middle) and ESF (right) galaxies. Shaded areas include 68% of the values. Median profiles for each galaxy are shown as coloured circles. *Bottom left:* median profiles normalized by their maximum value and fit to a Sérsic law. *Bottom right:* Median profile for ESF galaxies fit with two Sérsic components.

4 Star Formation Histories of CQ, CSF and ESF galaxies

For each galaxy, the SFH within the global elliptical aperture was built from the age, τ and mass values corresponding to the best cluster of solutions (Fig. 4 *left*). The median SFH of each galaxy type (Fig. 4 *right*) was calculated from the SFHs of the galaxies in each subsample.

According to this, CQ galaxies were the first to start their star formation (~ 1 Gyr ago). They would have had a very fast and violent star formation peak ~ 0.7 Gyr ago with a SFR of ~ 300 $M_\odot$/yr, being practically dead at present. CSF galaxies would have begun their SFH ~ 0.7 Gyr ago and their SFR would have been decreasing since then, except for some minor star formation burst in the last 200 Myr. In contrast, the ESF galaxies would have formed their stars more recently (in the last ~ 500 Myr) and their SFR would be approximately constant (~ 100 $M_\odot$/yr) since 200 Myr ago (or slightly decreasing at the moment).

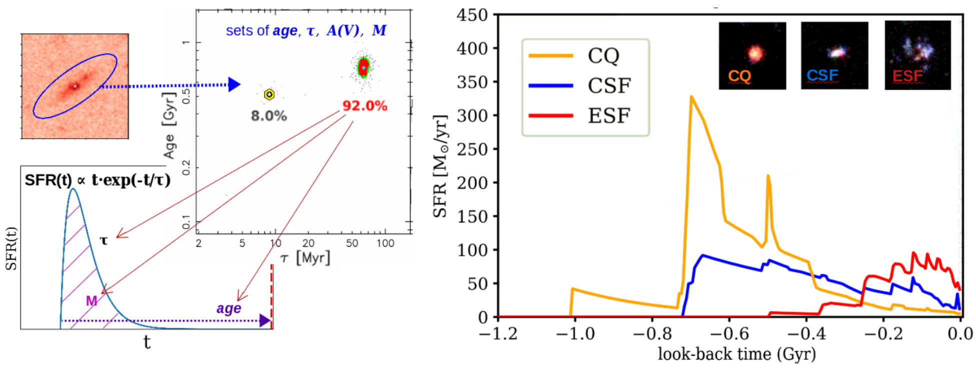

Figure 4: *Left:* Methodology: SFHs were built from the age, τ and mass values corresponding to the best cluster of solutions in the age$-\tau$ plane for the elliptical aperture of each galaxy. *Right:* Median SFH for each galaxy type: CSF (blue), CQ (orange) and ESF (red) galaxies.

5 Discussion: linking blue and red nuggets

Taking into account both the azimutally averaged surface stellar density profiles and the SFHs of each galaxy type, we could establish a possible evolutionary link among the three galaxy types. In the first place, the fact that CQ and CSF galaxies show very similar mass profiles could be explained assuming that CSF galaxies slowly die (or are already dying) keeping their structure until they become CQ galaxies. This would explain why CQ galaxies show the oldest mass-weighted ages.

Secondly, ESF galaxies, with a younger stellar population, could be the progenitors of CSF and CQ galaxies. In order to become a CSF galaxy, ESF systems must have lost their outer discs and become compact spheroids with intense star formation: CSF galaxies. These latter systems would reach a quiescent state with an old stellar population: CQ galaxies.

6 Self-consistent spatially resolved stellar populations

We are currently improving our 2D stellar population analysis by using data at lower spatial resolution, but better spectral resolution, such as photometric data from the SHARDS survey (OSIRIS@GTC) or spectrocopic data from HST grism. The left panel of Fig. 5 shows a zoom in the SHARDS zone for the sum of the spectra of each box in the photometric grid (cyan), aperture-corrected using the integrated photometry values for our HST bands (blue circles). The stars are photometric data we have measured for that galaxy in the SHARDS bands.

Our current work is focused on making this sum of the spectra of the boxes in the grid consistent, not only with the photometric values of SHARDS, but also with the spectrum measured for the whole galaxy using the HST grism shown in the right panel of Fig. 5, or, in the future, with ALMA data. Therefore, we would have access to, for example, both absorption and emission lines to constrain our SED-fits.

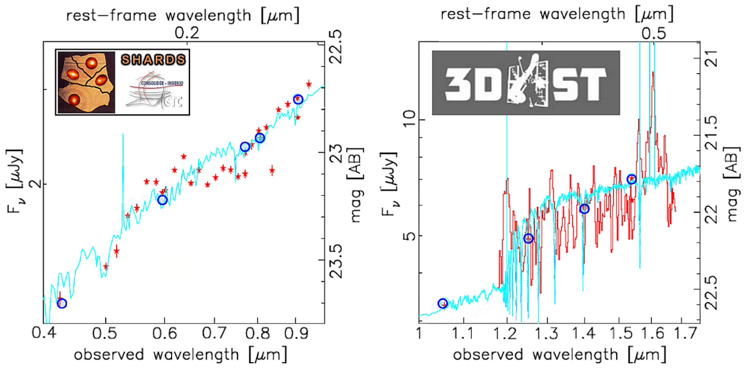

Figure 5: *Left:* zoom in the SHARDS filters spectral range. Sum of the spectra of the boxes in the grid (cyan) for galaxy GDN-25066, aperture-corrected with integrated photometry values of HST bands (blue circles). Red stars are photometric data in the SHARDS bands. *Right:* spectrum of the whole galaxy from the HST grism. Emission-lines are clearly detected. These lines could be used to constrain the properties of the most recent star formation in our SFHs.

References

[1] Barro, G., Faber, S. M., Pérez-González, P. G., et al. 2013, ApJ, 765, 104

[2] Bruzual G., Charlot S., 2003, MNRAS, 344, 1000

[3] Calzetti, D., Armus, L., Bohlin, R. C., et al. 2000, ApJ, 533, 682

[4] Chabrier, G. 2003, ApJ, 586, L133

[5] Cimatti A., et al., 2004, Nature, 430, 184

[6] Domínguez Sánchez H., Pozzi F., Gruppioni C. e. a., 2011, MNRAS, 417, 900

[7] Dressel, L., 2010. "Wide Field Camera 3 Instrument Handbook, Version 3.0" (Baltimore: STScI)

[8] Maybhate, A., et al. 2010, "ACS Instrument Handbook", Version 10.0 (Baltimore: STScI)

[9] Muzzin A., et al., 2013, ApJ, 777, 18

[10] Noeske K. G., Weiner B. J., Faber S. M. e. a., 2007, ApJ, 660, L43

[11] Pozzetti L., et al., 2010, A&A, 523, A13

[12] Sérsic, J. L. 1968, *Atlas de galaxias australes*, Universidad de Córdoba